Molecular BioSystems

A deterministic oscillatory model of microtubule growth and shrinkage for differential actions of short chain fatty acids

Journal:	*Molecular BioSystems*
Manuscript ID	MB-ART-03-2015-000211.R3
Article Type:	Paper
Date Submitted by the Author:	n/a
Complete List of Authors:	Kilner, Josephine; University of Sheffield, Corfe, Bernard; University of Sheffield, Department of Oncology McAuley, Mark; University of Chester, Wilkinson, Stephen; University of Chester,

SCHOLARONE™
Manuscripts

Molecular Biosystems

RSCPublishing

ARTICLE

A deterministic oscillatory model of microtubule growth and shrinkage for differential actions of short chain fatty acids

Cite this: DOI: 10.1039/xoxxoooooox

Received ooth January 2012,
Accepted ooth January 2012

DOI: 10.1039/xoxxoooooox

www.rsc.org/

Josephine Kilner [a], Bernard M. Corfe [b,c,†] Mark T. McAuley[d], Stephen J. Wilkinson [a,d]

Short chain fatty acids (SCFA), principally acetate, propionate, butyrate and valerate, are produced in pharmacologically relevant concentrations by the gut microbiome. Investigations indicate that they exert beneficial effects on colon epithelia. There is increasing interest in whether different SCFAs have distinct functions which may be exploited for prevention or treatment of colonic diseases including colorectal cancer (CRC), inflammatory bowel disease and obesity. Based on experimental evidence, we hypothesised that odd-chain SCFAs may possess anti-mitotic capabilities in colon cancer cells by disrupting microtubule (MT) structural integrity *via* dysregulation of β-tubulin isotypes. MT dynamic instability is an essential characteristic of MT cellular activity. We report a minimal deterministic model that takes a novel approach to explore the hypothesised pathway by triggering spontaneous oscillations to represent MT dynamic behaviour. The dynamicity parameters *in silico* were compared to those reported *in vitro*. Simulations of untreated and butyrate (even-chain length) treated cells reflected MT behaviour in interphase or untreated control cells. The propionate and valerate (odd-chain length) simulations displayed increased catastrophe frequencies and longer periods of MT-fibre shrinkage. Their enhanced dynamicity was dissimilar to that observed in mitotic cells, but parallel to that induced by MT-destabilisation treatments. Antimicrotubule drugs act through upward or downward modulation of MT dynamic instability. Our computational modelling suggests that metabolic engineering of the microbiome may facilitate managing CRC risk by predicting outcomes of SCFA treatments in combination with AMDs.

Introduction

Colorectal cancer (CRC) is the fourth most common cancer and second leading cause of cancer-related death in the UK.[1] Short chain fatty acids (SCFA) are closely associated with colon epithelia as by-products of anabolic fermentation by gut bacteria.[2] The principle SCFAs in the human gut are acetate, propionate, butyrate and valerate. These differ in carbon chain lengths (2, 3, 4 & 5 carbons, respectively). Butyrate is the most researched to date for colon health. It is the preferred energy source for the colonocyte, a potent regulator of cell fate,[3] particularly apoptosis,[4,5] and is thought to be chemopreventive. SCFAs have been shown to induce acetylation of target proteins, either *via* histone deacetylation[6,7] or by shifting the balance of acetyl-CoA reactions towards acetylation;[6,7] however, the mechanistic details of their functions in colonocytes are unclear. Our previous empirical work and others[6,8] suggested that carbon chain length may impact on their actions, with odd and even carbon-length SCFAs possessing distinct functions by virtue of different pathways in β-oxidation and entry into the TCA cycle.

Microtubules (MT) are cytoskeletal proteins that perform many critical cellular functions. In addition to maintaining cell structure, motility, intra- and intercellular transport, they are central to accurate formation and control of the mitotic spindle during cell division. MT fibres are composed of typically 13 protofilaments arranged longitudinally, each of which is constructed from αβ-tubulin heterodimers arranged in a head-to-tail manner. This confers the MT fibre with polarity so that polymerisation primarily occurs at the plus end. During assembly, the α-tubulin subunits are bound within the fibre and inaccessible to external proteins; conversely, the β-tubulin subunits are exposed on the surface enabling them to undergo post-translational modifications (PTM) and interact with microtubule associated proteins (MAP), including dynein and kinesin motor proteins. The arrangement of β-tubulin isotypes along the fibre combined with their PTMs has been hypothesised to generate a

tubulin code that may direct MT functions and regulate MT behaviour.[9,10] In order to perform their molecular functions MTs require the ability to rapidly grow, shrink and change direction in response to cellular cues. These transitions are an essential characteristic of MTs and are termed dynamic instability. The accepted view of MT dynamic instability is the MT capping model.[11] Briefly, phosphorylated αβ-tubulin dimers bind to the plus end of the MT fibre to form a protective tubulin-GTP cap. Immediately following polymerisation, the β-tubulin-GTP subunits undergo irreversible hydrolysis to their GDP form. Although this provides the necessary energy to drive MT growth,[12] β-tubulin-GDP is unstable and the fibre will rapidly dissociate if the protective GTP cap is not sustained. This is termed catastrophe and occurs when the pool of αβ-tubulin-GTP subunits in the vicinity of the fibre tip falls below a critical concentration.[13] Once released into the cytosol, β-tubulin-GDP subunits are free to rephosphorylate, restoring the critical concentration and enabling MT growth to resume, termed rescue. These actions are illustrated in Figure 1A. Experimental evidence on MT dynamics has primarily been derived from fluorescent tracking microscopy of growing and shrinking MTs *in vitro*.[14-18] The life history of an MT within a cell can range from several minutes to hours and involves extended periods of slow growth, short periods of rapid shrinkage and time spent pausing. Each period of elongation and shortening can consist of multiple catastrophes and rescues (Fig. 1B).[17,18] Despite appearing random, MT dynamic instability is a tightly regulated and orchestrated process.

Polymerisation of a β-tubulin GTP subunit to an MT fibre and its subsequent hydrolysis is a cooperative procedure. Suggested mechanisms include chemical and protein-protein interactions between β-tubulin GTP and GDP subunits;[19] conformational changes arising from GTP hydrolysis;[20] and facilitated diffusion. The latter mechanism postulated that αβ-tubulin dimers are transported towards the plus end of an MT fibre by virtue of fibre's polarity; as such, the probability that a dimer encounters an MT will increase as the MT lengthens.[21]

The β-tubulin superfamily comprises of six principle classes thought to have functional significance.[22,23] Most β-tubulin isotypes are species, tissue or cell type specific. Their relative proportions within an MT fibre can be regulated by upstream signalling events, suggesting they may influence MT functional activity.[24] Consequently, disrupting the fine balance of β-tubulin isotypes can lead to aberrant tubulin behaviour and may have implications in the progression of colonic diseases, including CRC.[18,24]

Our proteomic analyses investigated proteins differentially regulated in colon cancer cells by treatment with butyrate, propionate and valerate. The results identified several cytoskeletal proteins that were significantly dysregulated:[25] all three SCFAs targeted keratin 19; butyrate and propionate targeted actin; and propionate primarily targeted keratins 8 and 18; however, only propionate and valerate significantly targeted β-tubulin isotypes β2c-, β3- and β1-tubulin. These findings were consistent with our high content analyses (HCA) that had revealed valerate and propionate were the most effective in inducing MT breakdown and G2/M cell cycle arrest, despite being weaker effectors in apoptotic functions.[5,26] Whereas butyrate induces cytoskeletal breakdown *via* apoptosis,[4,5] these observations suggested that propionate and valerate may act through different mechanisms. Based on this evidence, it was hypothesised that odd- and even-chain SCFAs possessed distinct and unique metabolic functions.

SCFAs act by promoting post-translational acetylation of target proteins. Bioinformatic searches of Reactome and SABiosciences[24,27,28] indicated that the activities of several transcriptional regulators (TR) associated with β2c-, β3- and β1-tubulin genes (*RFX, PPAR, NSFR* and *NF-κB*) could be altered by acetylation. Histone acetylation also induces chromatin remodelling to promote transcription of target genes and can itself be influenced by upstream acetylation events.[29,30] These results suggested that treatment of colonocytes with SCFAs altered the regulation of specific genes, including overexpression of β2c- and β3-tubulin and suppression of β1-tubulin transcription *via* acetylation of *NF-κB*.[31,32] Both β2c- and β3-tubulin have been implicated in MT destabilisation;[24] although less is known about the role of β1-tubulin in MT dynamics.

Computational modelling has contributed to a better understanding of MT functions[20,33-36] and the biophysical details of MT dynamic instability. Various approaches have been adopted, including Monte Carlo simulations;[20,33] simplified coarse-grained stochastic models;[35] one- and three-dimensional modelling;[37] and models focusing on different types of lattices and MT fibre-fibre interactions.[33,36] The term "structural plasticity" invokes mechanisms more dependent on the structural conformations of bound subunits than their chemical states.[19] Simulated systems of dynamic MTs have also advanced understanding of their associations with MAPs, the collective behaviour of MTs and motors, and have been used to replicate mitotic events.[38,39] The model of Bayley *et al*. (1990. was pivotal in demonstrating the validity of the lateral-cap model, in which β-tubulin-GTP assembly is a cooperative stochastic event that is fully coupled with β-tubulin hydrolysis.[40] Their hypothesis was supported by Pedigo and Williams (2002) who showed that conformational changes arising from β-tubulin-GTP hydrolysis directly after association was best described using kinetic principles of lattice interactions.[20] Computational models have been proposed as a basis for predicting the actions of antimicrotubule drugs (AMDs).[40,41] This had particular relevance for our investigation which aimed to explore the links between SCFAs, transcriptional regulation of β-tubulin isotypes, MT integrity and performance, and the potential use of SCFAs in adjuvant therapies in CRC.

A common approach to modelling systems of this nature is to use ordinary differential equations (ODEs). These present biological systems as continuous and deterministic and assume that randomness is not an important factor in the system of interest. An alternative approach is to use stochastic models if there is deemed to be inherent variability within the biological system; a stochastic approach will be used in scenarios whereby a small number of molecules are suggested to be involved in discrete random collisions, such as during the expression of a single gene. The main limitation of stochastic models is that they have a tendency to be computationally intensive, as reviewed in McAuley *et al*. (2013).[42] In this study, we sought to develop a minimal deterministic model based on experimental evidence that might explain or validate our hypothesis:[25] that different SCFAs imposed differential effects on the balance of β-tubulin isotypes and their impact on MT integrity. A comparison between the stochastic behaviour of MTs *in vivo* and *in vitro* and a deterministic representation *in silico* is presented in Figure 1B and C.

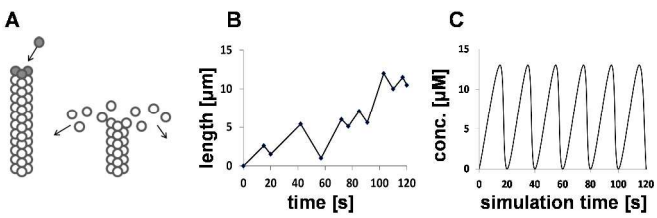

This journal is © The Royal Society of Chemistry 2012

Figure 1. Qualitative, Stochastic and deterministic representations of MT dynamic instability. (A) *(left) A growing MT fibre showing the protective cap (dark circles) formed from αβ-tubulin dimers with β-tubulin-GTP subunits; (right) an MT fibre undergoing catastrophe showing rapidly dissociating dimers with hydrolysed β-tubulin-GTP subunits (white circles).* ***(B)*** *The stochastic nature of MT dynamic instability in vivo and in vitro showing the life history of a growing MT as a series of catastrophe and rescue events.* ***(C)*** *A deterministic representation of MT dynamic instability in silico showing* regular periodic cycles in MT growth and shrinkage without the need for random perturbations.

2 Methods, kinetic theory and simulations

2.1 Qualitative model and design

The rationale underpinning the selection of a deterministic model made up of ODEs was based on our experimental observations. These had demonstrated that this system was deterministic and the inherent variability was negligible. The schematic diagram in Figure 2 shows the key events in the hypothesised pathway. Two scenarios are presented: the first represents untreated cells displaying normal MT behaviour (Fig. 2A); the second represents SCFA-treated cells promoting perturbation of MT dynamic instability (Fig. 2B). The first three reactions (k1–k3) are involved in the synthesis of the differentially regulated β-tubulin isotypes (β2c-, β3- and β1-tubulin); the next three reactions (k4–k6) are involved in MT dynamic instability based on the capping model.[11] With the exception of the perturbation step, the two parts of the model are distinct; therefore, no feedback loop has been included between the synthesis of *βeta* in the first part and the concentration of free β-tubulin subunits (tuGTP) in the second part. This was based on the assumption that the total number of β-tubulin subunits (free and bound) in the system is fixed but the relative proportions of stabilising and destabilising isotypes can shift. Consequently, the net upregulation of the three targeted β-tubulin isotypes (*βeta*) will be compensated by a net downregulation distributed among the remaining β-tubulin isotypes. (Based on our experimental results, none of the other β-tubulin isotypes was individually significantly downregulated).

The pathway in Figure 2B (treatment with odd-chain SCFAs) is described below:

- [k1–k3]: Treatment with odd-chain SCFAs drives acetylation of the target transcriptional regulators (TR); the acetylated TRs induce histone acetylation at β2c-, β3- and β1-tubulin genes (denoted βeta); thereby enhancing or extending synthesis of these β-tubulin isotypes.
- [k4–k6]: Free phosphorylated β-tubulin-GTP subunits co-operatively bind to the plus end of the MT fibre and are rapidly hydrolysed to their unstable β-tubulin-GDP form; dissociation of the MT fibre (catastrophe) releases the bound β-tubulin-GDP subunits back into the cytosol where they are re-phosphorylated, enabling MT re-polymerisation (rescue) to resume.
- The cycle then repeats.

The effect of raising the proportion of these three MT-destabilising β-tubulin isotypes in the system was to drive depolymerisation of the MT fibre, thereby inducing catastrophe. In contrast, untreated simulations or treatment with even-chain SCFAs (Fig. 2A) had little impact on the acetylation of target TRs, thereby preserving MT dynamic instability.

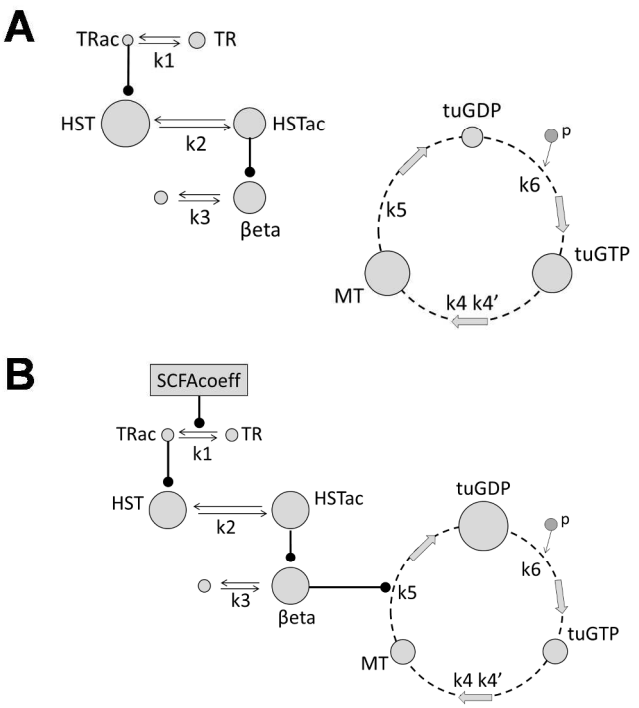

Figure 2. Schematic diagram representing the hypothesised effects of SCFA treatments on microtubule dynamic instability in colon cancer cells. *(A) Butyrate (an even-chain SCFA) has little or no impact on the regulatory pathway (k1→k3) leading to normal synthesis of the three target β-tubulin isotypes (βeta) relative to untreated cells. Therefore MT dynamic instability (k4→k6) remains unperturbed. (B) In contrast, treatment with propionate or valerate (odd-chain SCFAs) induces dysregulation of βeta leading to perturbation of MT dynamicity by promoting depolymerisation of the MT fibre (k6). Arrows show forward and backward reactions; round-ended arrows indicate the target reaction is promoted by the product of the preceding reaction; changes in the concentrations of reactants are represented by changes in the diameters of the circles. The following abbreviations are adopted: TR, transcriptional regulators; HST, histones at the target genes; βeta, the combined weighted fold-change of β3-, β2c- and β1- tubulin isotypes; MT, the MT fibre; tuGTP and tuGDP, total free phosphorylated and hydrolysed β-tubulin subunits, respectively; ac refers to the acetylated forms of TR and HST; p indicates phosphorylation; SCFAcoeff, the SCFA-activation coefficient specific to the hypothesised pathway.*

The modelled reactions obeyed kinetic rules and the relationships between the reactants were based on published observables and experimental data. Within the specifications of the modelled system, and due to the complexities of biological processes, each reaction in the pathway represented a number of intermediate sub-reactions. This approach of model reduction meant that the kinetic variables of the combined reactions could not be defined.[43] Reaction rates can also be altered by post-translational modifications.[44] As a result, parameters were set within biologically feasible limits derived from similar reactions reported in curated biomodels.[45] However, computational strategies have demonstrated that modelling can be successful in gaining valuable insights into biological mechanisms even under conditions where kinetic or reactant data are limited or unknown.[46,47]

2.2 Initial concentrations of reactants

The initial reactant concentrations are summarised in the Online Supplement (ESI, Table 1). Our proteomic data was used to define the steady state concentrations of *βeta* relative to untreated values, (1.07, 1.34 and 1.40 for butyrate, propionate and valerate, respectively). To match these values, the corresponding SCFA activation coefficients (SCFAcoeff) were manually adjusted to 1.2, 2.8, and 3.6, respectively. This is an accepted approach that has been described previously.[39] The total concentration of tubulin in the system was set at 10.0 μM based on typical values reported in the literature.[11,14,18,48] Although the concentrations of MTs, and bound and free β-tubulin subunits continually fluctuated, the overall concentration was assumed to be constant within the fixed volume of the *in silico* cell. Therefore, the initial concentrations could be arbitrarily set as MT = 5.5 μM; tuGDP = 3 μM; tuGTP 1.5 μM. These were informed estimates based on the nature of MT dynamic instability. Sensitivity analyses were performed to verify that the estimated values and assumptions were reasonable and appropriate, and to identify those parameters that would have the greatest impact of the model outcomes.

2.3 Kinetic rate laws and ODEs

The rate law interpretation was set as deterministic. The kinetic reactions, rate constants, rate laws and ODEs are summarised in the Online Supplement (ESI, Tables 2 and 3). The three steps of MT dynamic instability (β-tubulin phosphorylation, rescue and catastrophe; Fig. 2B) were inspired by Tyson's two-species model of cell division that displays spontaneous oscillations within set constraints.[49] This in turn had been based on the hypothetical model of a mitotic oscillator[50] and theoretical Brusselator model of chemical oscillations.[51,52] In this study we used a similar approach to construct a minimal oscillating model to describe MT dynamics in which the key requirement was for cooperative/non-linear kinetics within the cycle. By reducing MT dynamic instability to its three fundamental steps required us to ignore many of the additional levels of complexity, such as protein structure and memory effects.[53] Neglecting stochastic effects was also a major simplification even though the apparent randomness of dynamic instability is likely to be an important driving force in the true picture. However, the aim of this work was to show that cooperative kinetics for MT growth, dependant on a minimal concentration of free β-tubulin-GTP subunits, and a first order dissociation, could give credible results.

2.4 Simulations and output parameters

The key parameters of MT dynamicity are growth and shrinkage periods and rates and catastrophe and rescue frequencies; Catastrophe frequency is defined as the number of transitions from growth to shrinkage relative to the total elongation time; rescue frequency is defined as the number of transitions from shrinkage to growth relative to the total shrinkage time.[14,17] The time MTs spend pausing was beyond the scope of this model and not included in the analyses. As described earlier, an MT can undergo multiple sub-events of growth and shrinkage, catastrophes and rescues during its life history. These have been depicted as micro-oscillations.

The ratios of catastrophe:rescue frequencies, growth:shrinkage rates and growth:shrinkage times were calculated from the temporal data in order for equivalent comparisons to be made against the wide range of experimental data.

The simulations were undertaken in COPASI v4.7.[54] The simulation times ranged from 0 to 600–1000 s and data were recorded at intervals of 0.5 s. This provided a sufficient number of oscillations at a sensitivity suitable for analysis. The MT dynamicity parameters were evaluated following an initial delay of 500 s to allow β-tubulin synthesis to reach steady state (Fig. 3A).

3. Results

3.1 MT dynamicity parameters for SCFA treatments *in silico*

The inter-relationships between MT fibres and β-tubulin GTP and GDP subunits (MT, tuGTP and tuGDP, respectively; Fig. 3B): MT polymerisation commenced when the concentration of free tuGTP reached a critical concentration (cc); MT dissociation was triggered when the concentration of tuGTP fell below the cc; the subsequent decrease in MT concentration (representing length) was reflected by an increase in the concentration of free tuGDP. This model was based on the assumption that the concentration of free β-tubulin (tuGTP and tuGDP) was not constant but fluctuated in response to MT fibre growth and shrinkage. This implies that the concentration of free β-tubulin-GTP may play a role in MT dynamic instability. Although this supposition is relatively novel, it is not unprecedented: Janulevicius *et al*. (2006) explored this hypothesis through Monte Carlo simulations in the context of small cellular compartments and fluctuations in the concentration of free tubulin, and by extension, situations that affect the probability of MT association.[55] Their model was equated to neuronal growth cones *in vivo*; our model was based on changes in the local concentration of free β-tubulin-GTP at the fibre tip due to facilitated diffusion,[21] and thereby the probability of association.

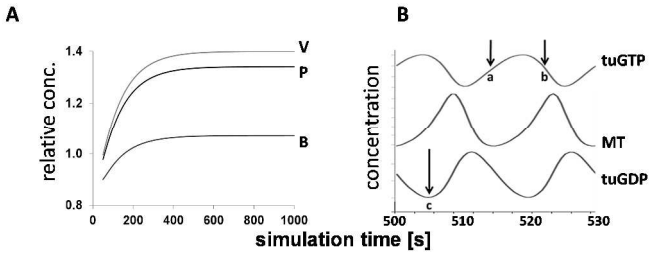

Figure 3. Temporal simulations showing the relationships between microtubule fibres and subunits in the hypothesised pathway. (A) *Treatment with propionate and valerate (odd-chain SCFAs) significantly promotes synthesis of target β-tubulin isotypes (βeta: β2c-tubulin, β3-tubulin, β1-tubulin); whereas butyrate has little influence on βeta synthesis relative to untreated cells. The curves show the relative concentrations of βeta following treatment with valerate (upper), propionate (centre) and butyrate (bottom). Steady state is achieved at approximately 500 s; the simulation time is 1000 s.* ***(B)*** *The stacked curves show the inter-relationships between MT fibres (MT, middle) free β-tubulin GTP and GDP subunits (tuGTP and tuGDP, top and bottom, respectively): the rapid gain and slow decline in free tuGDP is reflected by a rapid loss and slow increase in free tuGTP and consequently rapid shrinkage (catastrophe) and slow growth (rescue) in MT fibres; (a) indicates the point of rescue; (b) and (c) denote the critical concentration of tuGTP at which the protective cap at the end of the MT fibre is established and lost, respectively. Simulation time, 500–530 s.*

The temporal simulations for MTs for each SCFA treatment are shown in Figure 4A. The mean periods of the micro-oscillations were approximately 20 s. This was consistent with published values *in vitro* and *in vivo* for fluorescently tagged MTs.[17,18,56] Qualitative examination of the profiles showed that there was little difference between MT dynamicity in untreated cells *in silico* and those treated with butyrate (Fig. 4A). In both cases, the cycle of dynamic instability persisted over the simulation time and the mean concentration of MTs was 94% for butyrate relative to untreated values. In contrast, the MT profiles for propionate and valerate treatments showed increasing dampening of the oscillations, reflecting suppression of MT dynamic instability, and a reduction in

 This journal is © The Royal Society of Chemistry 2012

the mean concentrations of MTs to 74% and 71% relative to untreated values, respectively. Figure 4B shows the corresponding rate-profiles in untreated cells and valerate treated cells. These include the rates of concentration changes for MTs and free GTP and GDP β-tubulin subunits. Together, these results demonstrated that odd- and even-chain SCFAs induced distinct actions on MT dynamic instability. The odd-chain SCFAs effectively abolished MT dynamic instability *in silico*, reflecting dissociation of the fibres and loss of MT integrity *in vitro*, consistent with our experimental iTRAQ and HCA observations in HCT116 colon cancer cells. Comparisons between the simulated MT-dynamicity values for the three SCFAs relative to untreated values (Table 1) showed that the catastrophe frequencies were increased, the rescue frequencies decreased, the growth:shrinkage times increased and the growth:shrinkage rates decreased in the order butyrate to propionate to valerate, with valerate having the greatest effect.

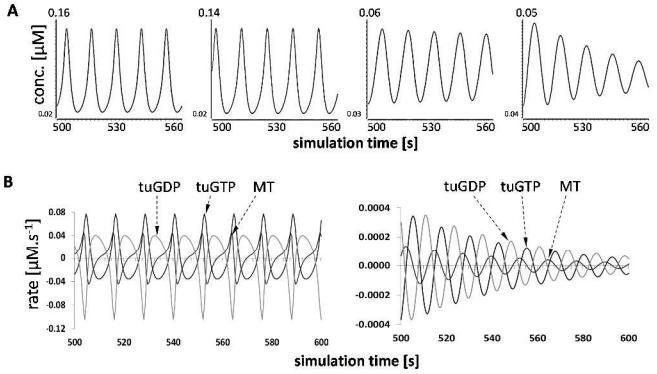

Figure 4. Temporal simulations showing MT dynamic behaviour under different SCFA treatments. (A) *Micro-oscillations depicting catastrophe and rescue events in simulated SCFA treatments during 60 s of the MT's lifespan: (left to right) untreated; butyrate (even-chain, 4 carbons); propionate (odd-chain, 3 carbons); and valerate (odd-chain, 5 carbons). There is little change in MT dynamicity between untreated and butyrate treated cells and MT dynamic instability persists over time; however, treatments with propionate and valerate reduce growth periods, increase shrinkage periods and suppress MT dynamic instability.* ***(B)*** *The rates of changes in MTs and free GDP and GTP β-tubulin (tuGDP and tuGTP) concentrations for untreated and valerate treated simulations show the predominance of second-order cooperative association in untreated MTs (left) and the shift towards first-order dissociation in valerate treated MTs (right).*

Table 1. Fold-changes in the MT-dynamicity parameters for simulated treatments with SCFAs relative to untreated values *in silico*.

MT Dynamicity parameter	Butyrate	Propionate	Valerate
catastrophe frequency [s-1]	0.98	1.08	1.24
rescue frequency [s-1]	0.97	0.83	0.72
catastrophe:rescue frequency	*1.01*	*1.29*	*1.73*
relative time growing	1.00	0.94	0.80
relative time shrinking	1.01	1.21	1.39
growth:shrinkage times	*0.99*	*0.77*	*0.58*
growth rate [μM/min]	0.92	0.13	0.001
shrinkage rate [μM/min]	0.91	0.10	0.000
growth:shrinkage rates	*1.01*	*1.29*	*1.45*

3.2 Comparisons between MT dynamicity parameters *in silico* and experimental data *in vitro*.

In order to determine whether the modelled outcomes could plausibly be attributed to MT destabilising treatments *in vitro*, they were compared to experimental measurements of MT dynamicity parameters in cells at different phases or undergoing different treatments. Experimental observations can yield a wide range of values for MT dynamicity dependent on species, tissue or cell type and external conditions; however they tend to report similar trends and ratios. For this reason, data from two representative reports were selected for interphase and mitotic epithelial cells,[17] and MT-destabilising and MT-stabilising treatments in epithelial cells[18] to minimise compounding effects. The experimental values are summarised in the online supplement (ESI, Table 4). The histograms in Figure 5 indicate that MT dynamicity ratios in untreated and butyrate treated cells *in silico* most closely matched those in interphase cells *in vitro* for growth and shrinkage but were closer to stabilised-control cells for catastrophe and rescue frequencies (Fig. 5A). Whereas, propionate and valerate treated MTs *in silico* displayed similarities to both mitotic and destabilised MTs *in vitro* for growth and shrinkage times and rates, but only to MT-destabilising treatments for catastrophe and rescue frequencies (Fig. 5B). Both mitotic and depolymerising MTs are dynamically active; however, these simulations strongly suggested that colon cancer cells treated with odd-chain SCFAs undergo MT-destabilisation as opposed to enhanced mitosis. These results supported our proposition that odd-chain SCFAs at above physiological concentrations may act as anti-microtubule agents

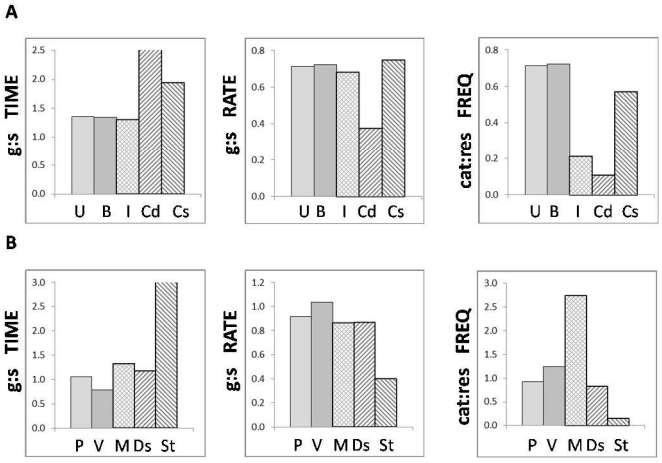

Figure 5. Goodness of fit of model to empirical data. *Comparisons between model predictions and published observations of MTs in vitro show that* ***(A)*** *simulations for untreated and butyrate (even-chain SCFA) treated MTs in silico most closely reflect those in interphase cells (I) for growth:shrinkage [g:s] periods and rates in vitro, and control cells in stabilising experiments (C-s) for catastrophe:rescue [cat:res] frequencies;* ***(B)*** *propionate and valerate (odd-chain SCFAs) treated MTs in silico most closely reflect MTs undergoing destabilising treatments (Ds) in vitro for all three MT dynamicity ratios; although they bear close similarities to mitotic cells (M) for growth:shrinkage periods and rates, they exhibit highly different behaviour from mitotic cells undergoing catastrophe and rescue. Note, the bars for growth:shrinkage times for Cd and St extend beyond the scale of the charts. [U, B, P, V: untreated, butyrate, propionate and valerate treatments in silico, respectively; I, M, Cs, Cd, St, Ds: interphase, mitotic, control cells for stabilising and destabilising treatments, stabilising and destabilising treatments in vitro, respectively.]*

3.3 Sensitivity analyses: Influences of initial concentrations and kinetic rate constants on model behaviour

Sensitivity analyses were carried out using the generic sensitivity framework in COPASI to assess the impacts of the initial reactant concentrations and kinetic rate constants on the reaction fluxes and temporal concentrations of the reactants, respectively. The summarised and scaled results are given in the Online supplement (ESI Table 5) and shown graphically in Figure 6A. The parameters with the greatest influences upstream of MT dynamic instability (k1→k3) were the initial concentration of histones (HST) and the forward kinetic rate constant for synthesis (k3f) of *βeta* (the three targeted β-tubulin isotypes): a 10% increase in the initial concentration of HST resulted in complete loss of MT dynamicity (Fig. 6B, centre); whereas a 10% increase in the forward rate of *βeta* synthesis led to over-stabilisation of the MTs (Fig. 6B, right), effectively negating the destabilising effects of valerate treatment (Fig. 6B, left). The dynamicity control factor that had the greatest influence in the cycle of MT dynamic instability was the rate of rephosphorylation of free tuGDP subunits (k6) (Fig. 6A).

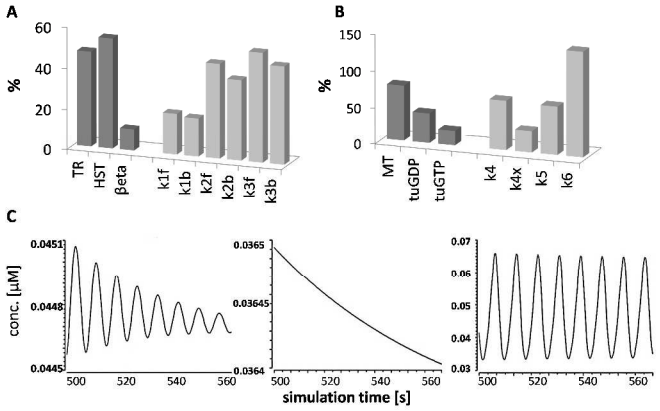

Figure 6. Sensitivity analyses showing the effects of small changes in the initial model parameters on the overall outcome of the model simulations. *The histograms show the summarised scaled sensitivities of the modelled system (y-axes) to changes in each of the initial reactant concentrations or kinetic reaction rates (x-axes) in* ***(A)*** *the βeta synthesis pathway and* ***(B)*** *the MT dynamic instability cycle. The dark coloured bars represent initial concentrations of the reactants; the pale coloured represent kinetic rates (k-rates). The results show that the initial concentration of histones (HST) and the forward rate of βeta synthesis (k3f) have the greatest influences on βeta synthesis; whereas the initial concentration of MTs and the rate of phosphorylation of free tuGDP (k6) have the greatest influences on MT dynamic instability.* ***(C)*** *Representative simulations of MTs undergoing valerate treatment showing the effects of 10% changes in the HST and k3f: (left) no change in either parameter; (centre) a 10% changes in the initial histone concentration (HST) leads to complete loss of MT dynamicity; (right) a 10% change in the forward rate of βeta synthesis (k3f) leads to overstabilisation of MT fibres. The effects of small changes in k6 are not shown due to the inherent instability of the oscillatory system not directly linked to SCFA input. There is no perturbation in untreated systems. The simulation times are 500–600 s.*

4. Discussion

Antimicrotubule drugs have proved highly successful in the treatment of multiple cancers and other diseases, such as motor neuron disease.[57,58] The review by Jordan and Wilson (2004) describes the ability of AMDs to induce apoptosis *via* mitotic arrest by suppressing MT dynamic instability.[59] It was also suggested that cancer cells may dysregulate expression of β-tubulin isotypes in order to enhance resistance to AMDs.[60] To date, SCFAs have not been directly identified as antimitotic agents, and experimental investigations have primarily focused on their ability to induce cell death and subsequent cytoskeletal breakdown *via* mechanisms that include alterations in pro- and anti-apoptotic proteins and tumour suppressor genes through Sp1 and Bcl-2 family proteins.[26,61] The importance of MAPs as the driving forces in dynamic instability is becoming increasingly evident.[55] This implies that the different β-tubulin isotypes also play critical roles through recruitment of MAPs. We previously reported that propionate and valerate, both odd-chain SCFAs, dysregulated the balance of β-tubulin isotypes towards those associated with MT depolymerisation, and that this was concurrent with impairment of MT structural integrity. To test the plausibility and potential implications of this hypothesis, we constructed a speculative model to explore the possible impact SCFAs might have on MT dynamic instability in colon cancer cells. The initial results showed that simulations of MT dynamic instability in untreated and butyrate treated cells *in silico* resembled MT behaviour observed in interphase or untreated control cells *in vitro*;[17] whereas simulations of propionate and valerate treatments (odd-chain SCFAs) showed close similarities to MTs under destabilising treatments *in vitro*.[18] The perturbation target for SCFA input in the model was set at the dissociation step of MT dynamic instability; therefore, increased levels of catastrophe relative to rescue had been anticipated. However, the key finding of this study was that the simulated outcomes were closer to those reported for MT-destabilising treatments *in vitro* than mitotic cells, despite both being associated with high levels of MT dynamicity. This demonstrated that propionate and valerate may possess anti-mitotic functions and suggested a potential role for odd-chain SCFAs as anti-mitotic agents, enabling AMDs to be administered at sub-optimal doses while maintaining efficacy and inhibiting resistance.

5. Conclusions

In combination with earlier experimental results,[25] the model presented here supports the hypothesis that propionate and valerate at supraphysiological concentrations trigger an anti-mitotic pathway in colon cancer cells that is unique to odd-chain SCFAs: the simulations provoked changes in MT dynamicity parameters that closely paralleled trends reported in cells undergoing MT-destabilising treatments.[18] This study has demonstrated that computational dynamic modelling can make a valuable contribution to such investigations, including the role of SCFAs in the treatment of CRC.

Acknowledgements

JK was supported by an EPSRC studentship (under grant EP/E036252/1)

Notes and references

[a] Biological and Systems Engineering Group, ChELSI Institute, Department of Chemical and Biological Engineering, University of Sheffield S1 3JD, UK.

[b] Molecular Gastroenterology Research Group, Academic Unit of Surgical Oncology, Department of Oncology, University of Sheffield, The Medical School, Beech Hill Road, Sheffield S10 2JF, UK;

[c] Insigneo Institute for *in silico* Medicine, Liversedge Building, University of Sheffield;

 This journal is © The Royal Society of Chemistry 2012

[d] Department of Chemical Engineering, University of Chester, Thornton Science Park, CH2 4NU, UK

† *Author for correspondence*: Dr Bernard Corfe, Molecular Gastroenterology Research Group, Academic Unit of Surgical Oncology, Department of Oncology, University of Sheffield, The Medical School, Beech Hill Road, Sheffield S10 2JF, UK. Email: b.m.corfe@shef.ac.uk Tel: +44 (0) 114 271 3004

Electronic Supplementary Information (ESI) available: [including literature-derived parameters used in development of the model]. See DOI: 10.1039/b000000x/

1. Cancer-Research-UK. Cancer Research UK: CancerStats Key Facts 2013 [Internet]. 2013 [cited 2013]. Available from: http://www.cancerresearchuk.org.
2. Cummings JH, Beatty ER, Kingman SM, Bingham SA, Englyst HN. Digestion and physiological properties of resistant starch in the human large bowel. Br J Nutr. 1996;75(5):733-47.
3. Augenlicht LH, Mariadason JM, Wilson A, Arango D, Yang WC, Heerdt BG, et al. Short chain fatty acids and colon cancer. J Nutr. 2002;132(12):3804S-8S.
4. Siavoshian S, Blottiere HM, Le Foll E, Kaeffer B, Cherbut C, Galmiche JP. Comparison of the effect of different short chain fatty acids on the growth and differentiation of human colonic carcinoma cell lines in vitro. Cell Biol Int. 1997;21(5):281-7.
5. Hinnebusch BF, Meng S, Wu JT, Archer SY, Hodin RA. The effects of short-chain fatty acids on human colon cancer cell phenotype are associated with histone hyperacetylation. J Nutr. 2002;132(5):1012-7.
6. Corfe BM. Hypothesis: butyrate is not an HDAC inhibitor, but a product inhibitor of deacetylation. Mol BioSyst. 2012;8:4.
7. Candido EP, Reeves R, Davie JR. Sodium butyrate inhibits histone deacetylation in cultured cells. Cell. 1978;14(1):105-13.
8. Astbury SM, Corfe BM. Uptake and Metabolism of the Short-Chain Fatty Acid Butyrate, a Critical Review of the Literature. Current Drug Metabolism. 2012;13(6):815-21.
9. Verdier-Pinard P, Pasquier E, Xiao H, Burd B, Villard C, Lafitte D, et al. Tubulin proteomics: towards breaking the code. Anal Biochem. 2009;384(2):197-206.
10. Verhey KJ, Gaertig J. The tubulin code. Cell Cycle. 2007;6(17):2152-60.
11. Drechsel DN, Hyman AA, Cobb MH, Kirschner MW. Modulation of the dynamic instability of tubulin assembly by the microtubule-associated protein tau. Mol Biol Cell. 1992;3(10):1141-54.
12. Desai A, Mitchison TJ. Microtubule polymerization dynamics. Annu Rev Cell Dev Biol. 1997;13:83-117.
13. Bonfils C, Bec N, Lacroix B, Harricane MC, Larroque C. Kinetic analysis of tubulin assembly in the presence of the microtubule-associated protein TOGp. J Biol Chem. 2007;282(8):5570-81.
14. Walker RA, Obrien ET, Pryer NK, Soboeiro MF, Voter WA, Erickson HP, et al. Dynamic instability of individual microtubules analyzed by video light-microscopy - rate constants and transition frequencies. J Cell Biol. 1988;107(4):1437-48.
15. Belmont LD, Hyman AA, Sawin KE, Mitchison TJ. Real-time visualization of cell cycle-dependent changes in microtubule dynamics in cytoplasmic extracts. Cell. 1990;62(3):579-89.
16. Cassimeris L. Accessory protein regulation of microtubule dynamics throughout the cell cycle. Curr Opin Cell Biol. 1999;11(1):134-41.
17. Rusan NM, Fagerstrom CJ, Yvon AMC, Wadsworth P. Cell cycle-dependent changes in microtubule dynamics in living cells expressing green fluorescent protein-alpha tubulin. Mol Biol Cell. 2001;12(4):971-80.
18. Kline-Smith SL, Walczak CE. The microtubule-destabilizing kinesin XKCM1 regulates microtubule dynamic instability in cells. Mol Biol Cell. 2002;13(8):2718-31.
19. Kueh HY, Mitchison TJ. Structural plasticity in actin and tubulin polymer dynamics. Science. 2009;325(5943):960-3.
20. Pedigo S, Williams RC. Concentration dependence of variability in growth rates of microtubules. Biophys J. 2002;83(4):1809-19.
21. Mechulam A, Chernov KG, Mucher E, Hamon L, Curmi PA, Pastre D. Polyamine Sharing between Tubulin Dimers Favours Microtubule Nucleation and Elongation via Facilitated Diffusion. Plos Computational Biology. 2009;5(1).
22. McKean PG, Vaughan S, Gull K. The extended tubulin superfamily. J Cell Sci. 2001;114(Pt 15):2723-33.
23. Luduena RF. Are tubulin isotypes functionally significant. Mol Biol Cell. 1993;4(5):445-57.
24. Leandro-Garcia LJ, Leskela S, Landa I, Montero-Conde C, Lopez-Jimenez E, Leton R, et al. Tumoral and Tissue-Specific Expression of the Major Human beta-Tubulin Isotypes. Cytoskeleton (Hoboken). 2010;67(4):214-23.
25. Kilner J, Waby JS, Chowdry J, Khan AQ, Noirel J, Wright PC, et al. A proteomic analysis of differential cellular responses to the short-chain fatty acids butyrate, valerate and propionate in colon epithelial cancer cells. Mol BioSyst. 2012;8(4):1146-56.
26. Heerdt BG, Houston MA, Augenlicht LH. Short-chain fatty acid-initiated cell cycle arrest and apoptosis of colonic epithelial cells is linked to mitochondrial function. Cell Growth Differ. 1997;8(5):523-32.
27. REACTOME: a manually curated and peer-reviewed pathway database. Reactome [Internet]. 2010 [cited 2012]. Available from: http://www.reactome.org.
28. Transcription Regulator Search Portal [Internet]. Qiagen Inc. USA [Internet]. 2010 [cited 2012 Aug 01]. Available from: http://www.sabiosciences.com/home.php.
29. Naruse Y, Aoki T, Kojima T, Mori N. Neural restrictive silencer factor recruits mSin3 and histone deacetylase complex to repress neuron-specific target genes. Proc Natl Acad Sci USA. 1999;96(24):13691-6.
30. Kurschat P, Bielenberg D, Rossignol-Tallandier M, Stahl A, Klagsbrun M. Neuron restrictive silencer factor NRSF/REST is a transcriptional repressor of neuropilin-1 and diminishes the ability of semaphorin 3A to inhibit keratinocyte migration. J Biol Chem. 2006;281(5):2721-9.
31. Chen LF, Greene WC. Assessing acetylation of NF-kappa B. Methods. 2005;36(4):368-75.
32. Crump NT, Hazzalin CA, Bowers EM, Alani RM, Cole PA, Mahadevan LC. Dynamic acetylation of all lysine-4 trimethylated histone H3 is evolutionarily conserved and mediated by p300/CBP. Proc Natl Acad Sci USA. 2011;108(19):7814-9.
33. Martin SR, Schilstra MJ, Bayley PM. Dynamic Instability of Microtubules - Monte-Carlo Simulation and Application to Different Types of Microtubule Lattice. Biophys J. 1993;65(2):578-96.
34. Hall D. The effects of Tubulin denaturation on the characterization of its polymerization behavior. Biophys Chem. 2003;104(3):655-82.
35. Gregoretti IV, Margolin G, Alber MS, Goodson HV. Insights into cytoskeletal behavior from computational modeling of

dynamic microtubules in a cell-like environment. J Cell Sci. 2006;119(Pt 22):4781-8.
36. Karsenti E, Nedelec F, Surrey T. Modelling microtubule patterns. Nature Cell Biology. 2006;8(11):1204-11.
37. Brun L, Rupp B, Ward JJ, Nedelec F. A theory of microtubule catastrophes and their regulation. Proc Natl Acad Sci USA. 2009;106(50):21173-8.
38. Ibrahim B, Diekmann S, Schmitt E, Dittrich P. In-silico modeling of the mitotic spindle assembly checkpoint. PLoS One. 2008;3(2):e1555.
39. Caydasi AK, Lohel M, Gruenert G, Dittrich P, Pereira G, Ibrahim B. A dynamical model of the spindle position checkpoint. Mol Syst Biol. 2012;8.
40. Bayley PM, Schilstra MJ, Martin SR. Microtubule dynamic instability - numerical-simulation of microtubule transition properties using a lateral cap model. J Cell Sci. 1990;95:33-48.
41. Buxton GA, Siedlak SL, Perry G, Smith MA. Mathematical modeling of microtubule dynamics: insights into physiology and disease. Prog Neurobiol. 2010;92(4):478-83.
42. McAuley MT, Proctor CJ, Corfe BM, Cuskelly GJ, Mooney KM. Nutrition Research and the Impact of Computational Systems Biology. J Comp Sci Syst Biol. 2013;6(5):271-85.
43. Wu J, Vidakovic B, Voit EO. Constructing stochastic models from deterministic process equations by propensity adjustment. BMC Syst Biol. 2011;5:187.
44. Cheung P, Tanner KG, Cheung WL, Sassone-Corsi P, Denu JM, Allis CD. Synergistic coupling of histone H3 phosphorylation and acetylation in response to epidermal growth factor stimulation. Mol Cell. 2000;5(6):905-15.
45. Li C, Donizelli M, Rodriguez N, Dharuri H, Endler L, Chelliah V, et al. BioModels Database: An enhanced, curated and annotated resource for published quantitative kinetic models. BMC Syst Biol. 2010;4:92.
46. Wilkinson SJ, Benson N, Kell DB. Proximate parameter tuning for biochemical networks with uncertain kinetic parameters. Molecular Biosystems. 2008;4(1):74-97.
47. Dimelow RJ, Wilkinson SJ. Control of translation initiation: a model-based analysis from limited experimental data. J R Soc Interface. 2009;6(30):51-61.
48. Caplow M, Shanks J. Induction of microtubule catastrophe by formation of tubulin - gdp and apotubulin subunits at microtubule ends. Biochemistry. 1995;34(48):15732-41.
49. Tyson JJ. Modeling the cell-division cycle - cdc2 and cyclin interactions. Proc Natl Acad Sci USA. 1991;88(16):7328-32.
50. Tyson J, Kauffman S. Control of mitosis by a continuous biochemical oscillation: Synchronization; spatially inhomogeneous oscillations. J Math Biol. 1975;1(4):289-310.
51. Prigogine I, Lefever, R. Symmetry breaking instabilities in dissipative systems. II. J Chem Phys. 1968;48(4):1695-700.
52. Tyson J. Some Further Studies of Nonlinear Oscillators in Chemical Systems. J Chem Phys. 1973;58:3919-30.
53. Brouhard GJ. Dynamic instability 30 years later: complexities in microtubule growth and catastrophe. Mol Biol Cell. 2015;26(7):1207-10.
54. Hoops S, Sahle S, Gauges R, Lee C, Pahle J, Simus N, et al. COPASI--a COmplex PAthway SImulator. Bioinformatics. 2006;22(24):3067-74.
55. Janulevicius A, van Pelt J, van Ooyen A. Compartment volume influences microtubule dynamic instability: a model study. Biophys J. 2006;90(3):788-98.
56. Bolterauer H, Limbach HJ, Tuszyński JA. Models of assembly and disassembly of individual microtubules: stochastic and averaged equations. J Biol Phys. 1999;25(1):1-22.
57. Don S, Verrills NM, Liaw TY, Liu ML, Norris MD, Haber M, et al. Neuronal-associated microtubule proteins class III beta-tubulin and MAP2c in neuroblastoma: role in resistance to microtubule-targeted drugs. Mol Cancer Ther. 2004;3(9):1137-46.
58. Singh P, Rathinasamy K, Mohan R, Panda D. Microtubule assembly dynamics: an attractive target for anticancer drugs. IUBMB Life. 2008;60(6):368-75.
59. Jordan MA, Wilson L. Microtubules as a target for anticancer drugs. Nat Rev Cancer. 2004;4(4):253-65.
60. Burkhart CA, Kavallaris M, Band Horwitz S. The role of beta-tubulin isotypes in resistance to antimitotic drugs. Biochim Biophys Acta. 2001;1471(2):O1-9.
61. Waby JS, Chirakkal H, Yu CW, Griffiths GJ, Benson RSP, Bingle CD, et al. Sp1 acetylation is associated with loss of DNA binding at promoters associated with cell cycle arrest and cell death in a colon cell line. Mol Cancer. 2010;9.

 This journal is © The Royal Society of Chemistry 2012

Figure 1

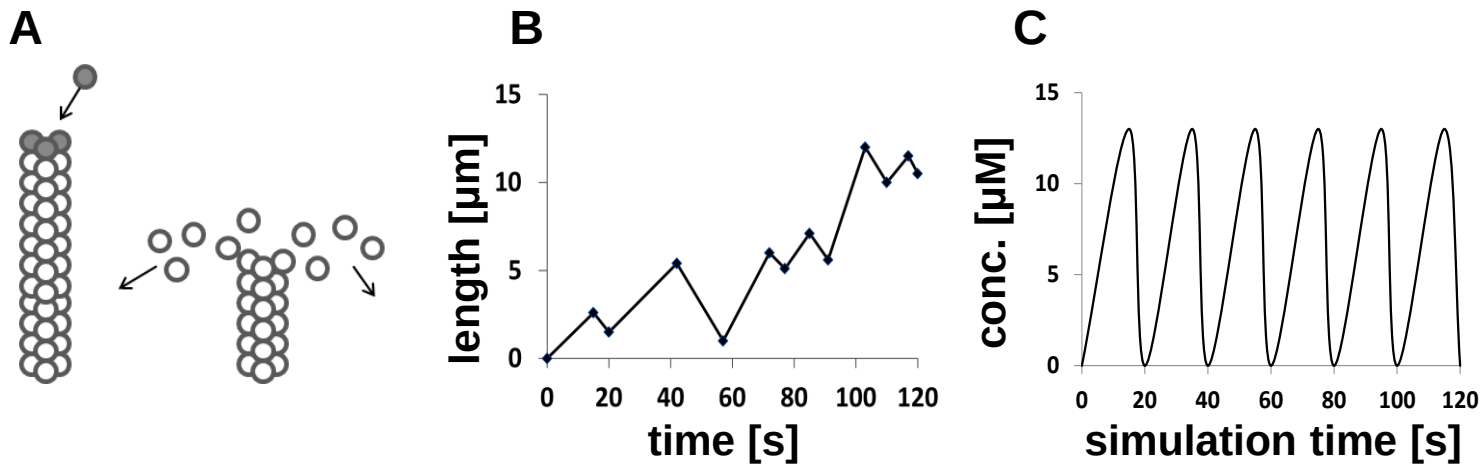
A
B
C
length [µm]
time [s]
conc. [µM]
simulation time [s]
0
5
10
15
0
20
40
60
80
100
120

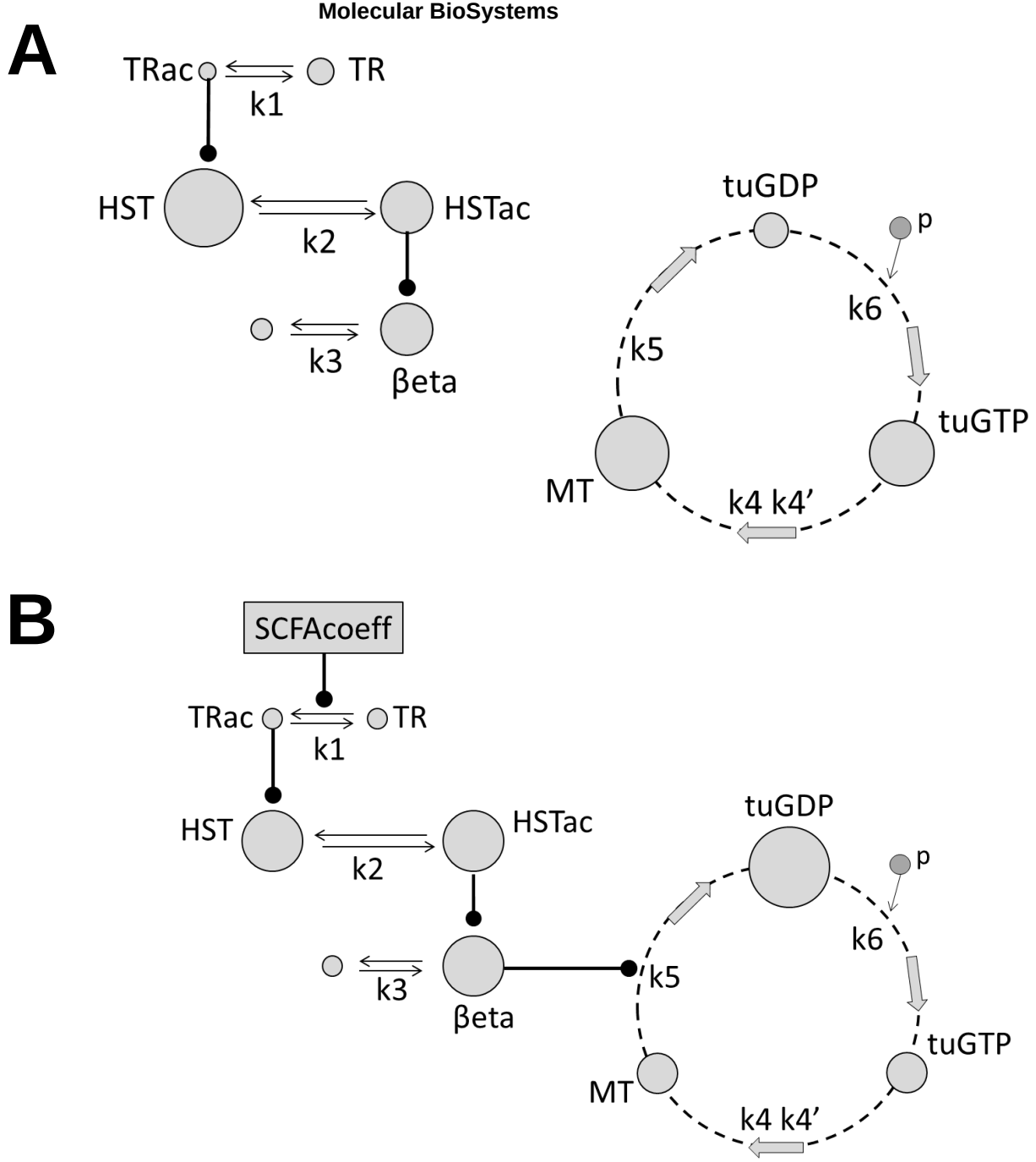
A
TRac
TR
k1
HST
HSTac
k2
k3
βeta
tuGDP
p
k6
k5
tuGTP
MT
k4 k4'
B
SCFAcoeff
TRac
TR
k1
HST
HSTac
k2
k3
βeta
tuGDP
p
k6
k5
tuGTP
MT
k4 k4'

Figure 3

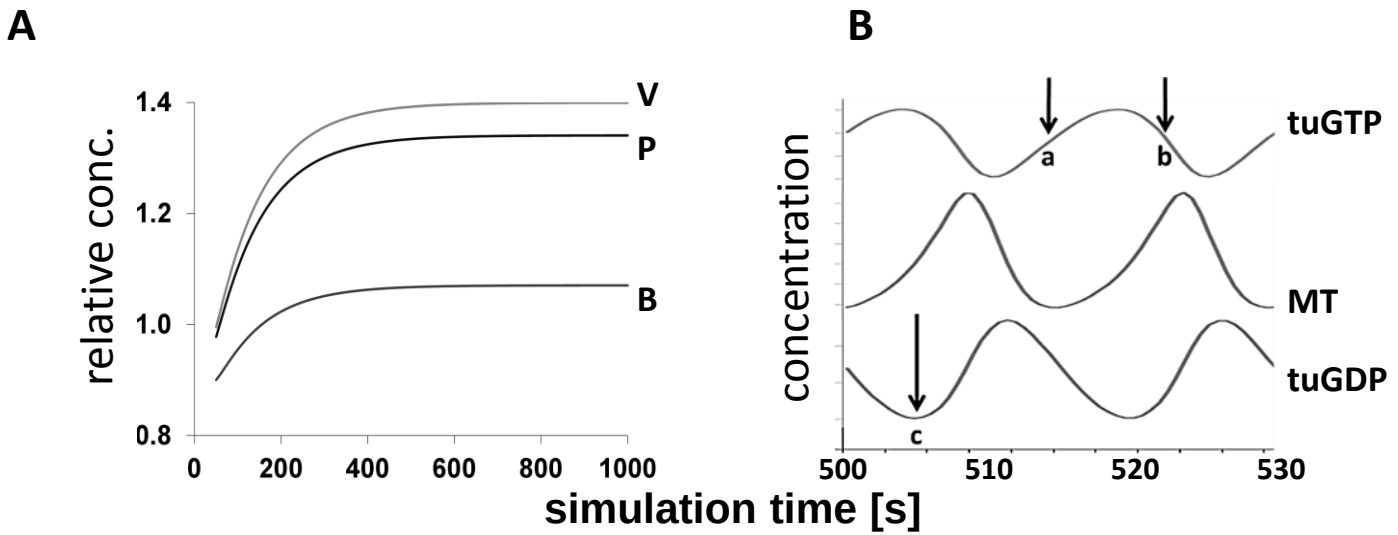
A
B
relative conc.
1.4
1.2
1.0
0.8
V
P
B
0
200
400
600
800
1000
concentration
a
b
c
tuGTP
MT
tuGDP
500
510
520
530
simulation time [s]

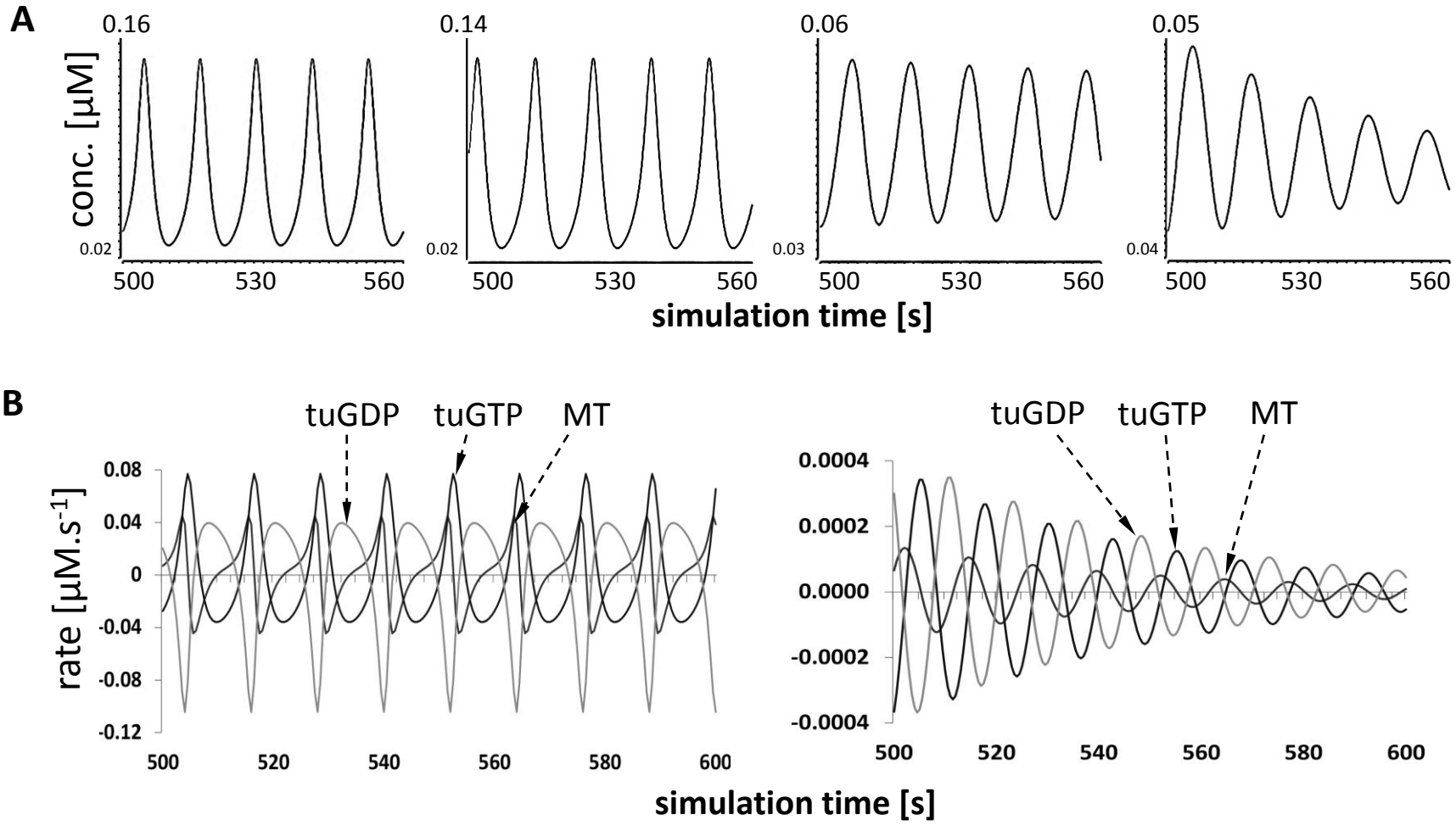
A
0.16
0.14
0.06
0.05
conc. [µM]
0.02
0.02
0.03
0.04
500
530
560
simulation time [s]
B
tuGDP
tuGTP
MT
rate [µM.s-1]
0.08
0.04
0
-0.04
-0.08
-0.12
0.0004
0.0002
0.0000
-0.0002
-0.0004
500
520
540
560
580
600
simulation time [s]

Figure 5

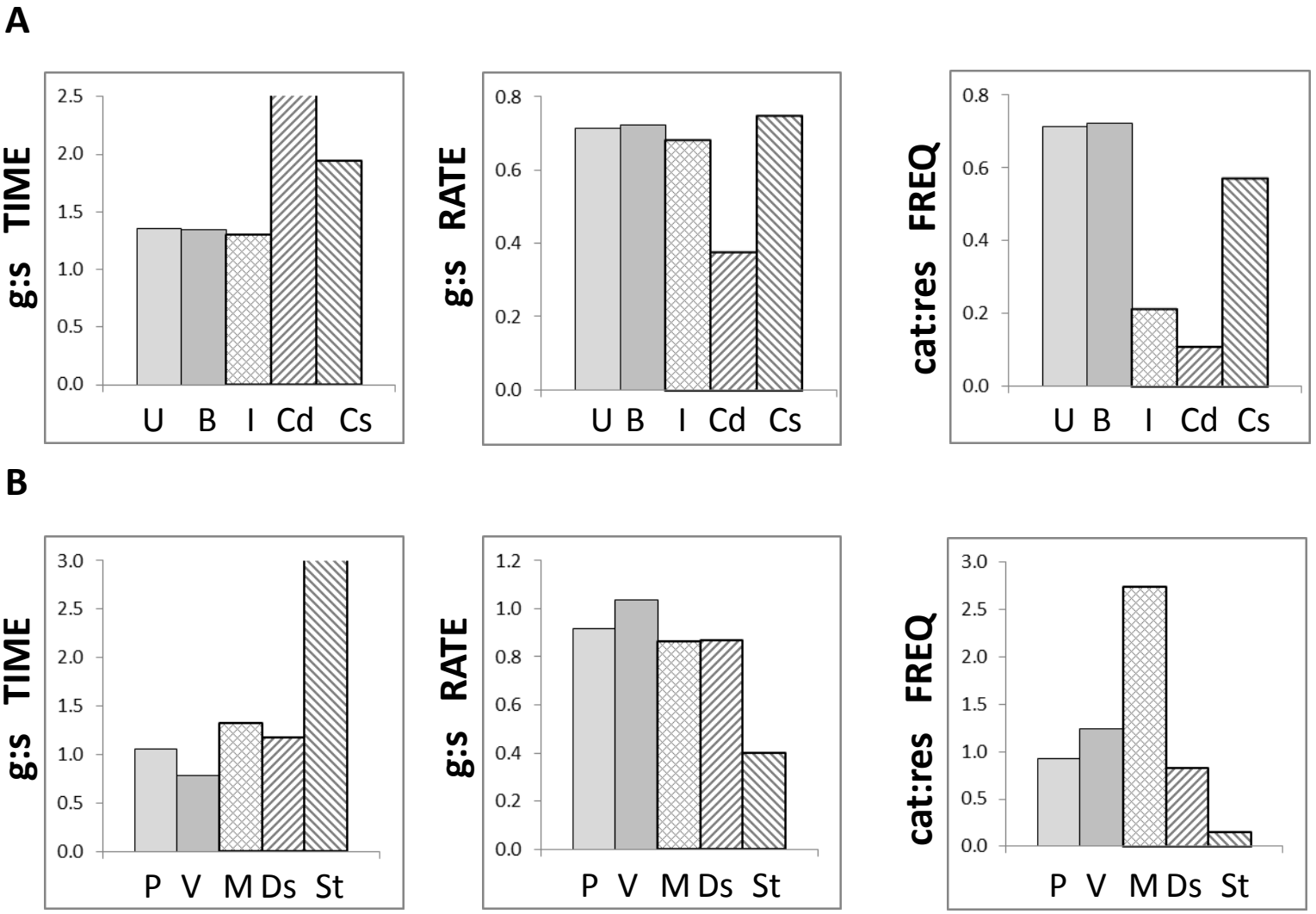
A
g:s TIME
2.5
2.0
1.5
1.0
0.5
0.0
U B I Cd Cs
g:s RATE
0.8
0.6
0.4
0.2
0.0
U B I Cd Cs
cat:res FREQ
0.8
0.6
0.4
0.2
0.0
U B I Cd Cs
B
g:s TIME
3.0
2.5
2.0
1.5
1.0
0.5
0.0
P V M Ds St
g:s RATE
1.2
1.0
0.8
0.6
0.4
0.2
0.0
P V M Ds St
cat:res FREQ
3.0
2.5
2.0
1.5
1.0
0.5
0.0
P V M Ds St

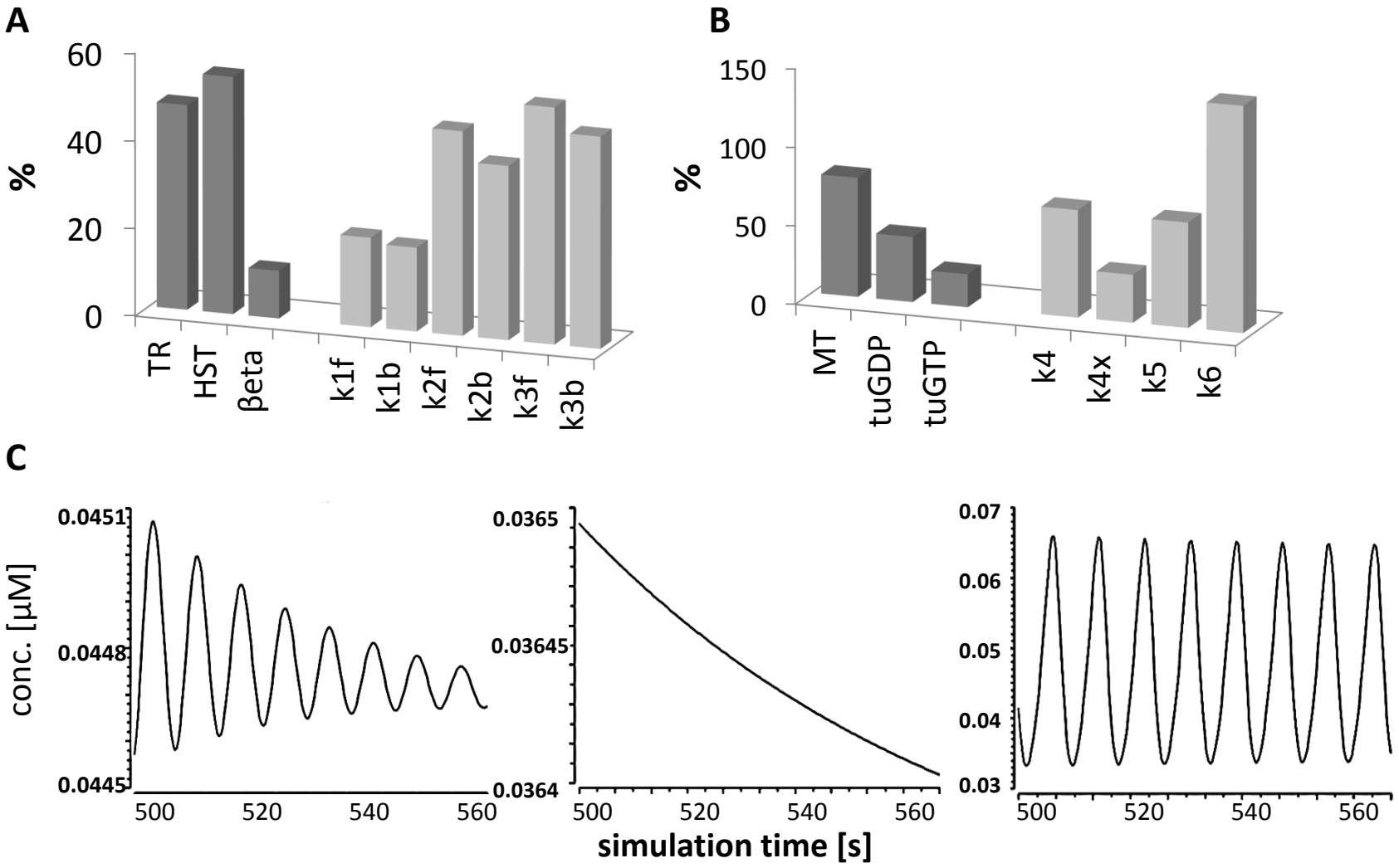
A
%
60
40
20
0
TR
HST
βeta
k1f
k1b
k2f
k2b
k3f
k3b
B
%
150
100
50
0
MT
tuGDP
tuGTP
k4
k4x
k5
k6
C
conc. [µM]
0.0451
0.0448
0.0445
0.0365
0.03645
0.0364
0.07
0.06
0.05
0.04
0.03
500
520
540
560
simulation time [s]

ESI Table 1. The initial reactant concentrations and source references.

Reactant	Initial concentration	Unit	Source references
SCFAcoeff	(1.00 → 3.60)	µM	*N/A*
TR	0.05	µM	[1,2]
TRac	0	µM	
HST	0.3	µM	[1,2]
HSTac	0	µM	
βeta	1.1	µM	[3]
MT	5.5	µM	[4-7]
tuGDP	3	µM	
tuGTP	1.5	µM	

ESI Table 2. The kinetic reactions, rate constants, rate laws and ODEs used in the modeled system.

Equation; activator	Rate constant	Rate law	ODE
TR → *TRac;* *SCFAcoeff*	k1f	irr. mass action, activated	d[*TRac*]/dt = - (k1b[*TRac*]) + (k1f [*TR*] [*SCFAcoeff*])
TRac → *TR*	k1b	irr. mass action	
HST → *HSTac;* *TRac*	k2f	irr. mass action, activated	d[*HSTac*]/dt = - (k2b[*HSTac*]) + (k2f [*HST*] [*TRac*])
HSTac → *HST*	k2b	irr. mass action	
→ *βeta;* *HSTac*	k3f	zero order, activated	d[*βeta*]/dt = - (k3b[*βeta*]) + (k3f [*HSTac*])
βeta →	k3b	irr. mass action	
tuGTP → *MT*	k4; k4x	non-linear second order	d[*MT*]/dt = - (k5[*MT*][*βeta*]) + ([*tuGTP*] (k4x + k4 [*MT*]^2))
MT → *tuGDP;* *βeta*	k5	irr. mass action, activated	d[*tuGDP*]/dt = - (k6 [*tuGDP*]) + (k5[*MT*][*βeta*])
tuGDP → *tuGTP*	k6	irr. mass action	d[*tuGTP*]/dt = - ([*tuGTP*] (k4x + k4 [*MT*]^2)) + (k6 [*tuGTP*])

irr: irreversible; f: denotes a forward reaction; b: denotes a backward reaction

ESI Table 3. The forward and reverse kinetic rate constants in the modelled pathway.

Reaction	Rate constant	Value	Units	Range	Source references
TR acetylation	k1f	0.30	$\mu M^{-1}s^{-1}$	0.2 to 5 s^{-1}	[1,8]
TR deacetylation	k1b	0.25	s^{-1}		
Histone acetylation	k2f	0.275	$\mu M^{-1}s^{-1}$	0.35 s^{-1} ; 0.3 s^{-1}	[9]
Histone deacetylation	k2b	0.05	s^{-1}		
βeta synthesis	k3f	0.23	s^{-1}	0.01–0.6 s^{-1}	[10,11]
βeta degradation	k3b	0.30	s^{-1}	0.06–2 s^{-1}	
MT rescue	k4	50			
	k4x	0.081	s^{-1}	upper & lower	[12]
MT catastrophe	k5	1	$\mu M^{-1}s^{-1}$	constraints	
tuGDP phosphorylation	k6	0.0065	s^{-1}		

f: denotes a forward reaction; b: denotes a backward reaction

ESI Table 4. Published experimental data for MT dynamicity parameters in **(A)** interphase cells and control cells for MT destabilising and stabilising treatments; **(B)** mitotic cells and cells undergoing MT-destabilising and MT-stabilising treatments.

(A)

MT dynamicity parameter	Interphase cells[a]	control cells (destabilising)[b]	control cells (stabilising)[b]
catastrophe frequency [s^{-1}]	0.023	0.004	0.012
rescue frequency [s^{-1}]	0.108	0.036	0.020
% time elongating	15.9	66.2	38.7
% time shortening	12.2	7.2	19.9
% time pausing	*72.0*	*28.9*	*39.4*
growth rate [µm. min^{-1}]	9.875	3.6	4.8
shrinkage rate [µm. min^{-1}]	14.50	9.5	6.4

(B)

MT dynamicity parameter	Mitotic cells[a]	MT-destabilised cells[b]	MT-stabilised cells[b]
catastrophe frequency [s^{-1}]	0.089	0.018	0.006
rescue frequency [s^{-1}]	0.033	0.021	0.038
% time elongating	50.5	34.1	63.8
% time shortening	38.1	29.0	7.6
% time pausing	11.4	38.7	29.0
growth rate [µm. min^{-1}]	13.12	6.0	4.0
shrinkage rate [µm. min^{-1}]	15.15	6.9	10.0

Mean values: [a] Rusan *et al*. (2001); [b] Kline-Smith & Walczak (2002) [6,13]

ESI Table 5. The sensitivities of the model outcomes to the initial parameters. The results show the summarised, scaled sensitivities: **(A)** the influences of the initial concentrations of the reactants on the reaction fluxes; **(B)** the influences of the kinetic rate constants on the temporal concentrations of the reactants.

A

Variable: initial concentration	**Target function: fluxes of reactions**
TR	46.73
HST	54.14
βeta	10.87
MT	75.86
tuGDP	41.43
tuGTP	21.03

B

Variable: kinetic rate constant	**Target function: temporal concentrations**
k1f (*TR*-acetylation)	20.40
k1b (*TR*-deacetylation)	19.13
k2f (*HST*-acetylation)	46.70
k2b (*HST*-deacetylation)	39.78
k3f (*βeta*-synthesis)	54.09
k3b (*β*eta-degradation)	48.44
k4 (rescue)	68.51
k4x (rescue-x)	30.62
k5 (catastrophe)	67.14
k6 (phosphorylation)	144.71

f: denotes a forward reaction; b: denotes a backward reaction

References

1. Chan C, Stark J, George AJT. Feedback control of T-cell receptor activation. Proc R Soc Lond Ser B: Biol Sci. 2004;271(1542):931-9.
2. Smolen P, Hardin PE, Lo BS, Baxter DA, Byrne JH. Simulation of Drosophila circadian oscillations, mutations, and light responses by a model with VRI, PDP-1, and CLK. Biophys J. 2004;86(5):2786-802.
3. Kilner J, Waby JS, Chowdry J, Khan AQ, Noirel J, Wright PC, et al. A proteomic analysis of differential cellular responses to the short-chain fatty acids butyrate, valerate and propionate in colon epithelial cancer cells. Mol BioSyst. 2012;8(4):1146-56.
4. Caplow M, Shanks J. Induction of microtubule catastrophe by formation of tubulin - GDP and apotubulin subunits at microtubule ends. Biochemistry. 1995;34(48):15732-41.
5. Drechsel DN, Hyman AA, Cobb MH, Kirschner MW. Modulation of the dynamic instability of tubulin assembly by the microtubule-associated protein tau. Mol Biol Cell. 1992;3(10):1141-54.
6. Kline-Smith SL, Walczak CE. The microtubule-destabilizing kinesin XKCM1 regulates microtubule dynamic instability in cells. Mol Biol Cell. 2002;13(8):2718-31.
7. Walker RA, Obrien ET, Pryer NK, Soboeiro MF, Voter WA, Erickson HP, et al. Dynamic instability of individual microtubules analyzed by video light-microscopy - rate constants and transition frequencies. J Cell Biol. 1988;107(4):1437-48.
8. Stoops JK, Singh N, Wakil SJ. The yeast fatty-acid synthase - pathway for transfer of the acetyl group from coenzyme a to the cys-sh of the condensation site. J Biol Chem. 1990;265(28):16971-7.
9. Cheung P, Tanner KG, Cheung WL, Sassone-Corsi P, Denu JM, Allis CD. Synergistic coupling of histone H3 phosphorylation and acetylation in response to epidermal growth factor stimulation. Mol Cell. 2000;5(6):905-15.
10. Chen KC, Calzone L, Csikasz-Nagy A, Cross FR, Novak B, Tyson JJ. Integrative analysis of cell cycle control in budding yeast. Mol Biol Cell. 2004;15(8):3841-62.
11. Schuetz A, Min J, Allali-Hassani A, Schapira M, Shuen M, Loppnau P, et al. Human HDAC7 harbors a class IIa histone deacetylase-specific zinc binding motif and cryptic deacetylase activity. J Biol Chem. 2008;283(17):11355-63.
12. Tyson JJ. Modeling the cell-division cycle - cdc2 and cyclin interactions. Proc Natl Acad Sci USA. 1991;88(16):7328-32.
13. Rusan NM, Fagerstrom CJ, Yvon AMC, Wadsworth P. Cell cycle-dependent changes in microtubule dynamics in living cells expressing green fluorescent protein-alpha tubulin. Mol Biol Cell. 2001;12(4):971-80.